Molecular Dynamics Studies of Cation Aggregation in the Room Temperature Ionic Liquid [C_{10}mim][Br] in Aqueous Solution†

B. L. Bhargava* and Michael L. Klein*

Center for Molecular Modeling, Department of Chemistry, University of Pennsylvania, 231 South 34th Street, Philadelphia, Pennsylvania 19104-6323

Received: August 1, 2008; Revised Manuscript Received: September 2, 2008

The structure of an aqueous 1-*n*-decyl-3-methylimidazolium bromide solution and its vapor−liquid interface has been studied using molecular dynamics (MD) simulations. Starting from an isotropic solution, spontaneous self-assembly of cations into small micellar aggregates has been observed. The decyl chains are buried inside the micelle to avoid unfavorable interactions with water, leaving the polar headgroups exposed to water. The cation aggregation numbers, ranging from 15 to 24 compare favorably with experimental estimates. Results are presented for the organization of solvent around the cations. The structure of the aggregates as determined from the present MD simulations does not support the staircase model proposed on the basis of nuclear magnetic resonance studies on similar aqueous ionic-liquid solutions. The distribution of ions in bulk solutions and at an air/water interface is also discussed.

1. Introduction

Room temperature ionic liquids (RTILs) are known to possess unique properties,[1,2] and due to their enormous potential for industrial applications,[3−5] they have been the subject of many experimental and computational investigations[6−9] over the past decade. RTILs based on the imidazolium cation have been particularly well studied.[10−18] The effect of adding water on the behavior of ionic liquids with short alkyl chain has been studied using MD simulations.[19] Several interesting changes in physical properties, such as faster diffusion of ions, have been observed. However, there have not been any computational studies on aqueous solutions of long alkyl chain ionic liquids. Experiments and MD studies have shown that long-chain alkylimidazolium compounds exhibit nanoscale segregation of the polar imidazolium cations, bromide anions, and nonpolar alkyl chains.[20−22] The segregation is more dramatic in the case of RTILs with longer alkyl chains, where hydrophobic interactions between the chains play a more important role in determining the structure of the liquid. Nonpolar hydrophobic alkyl groups are expected to be found at the liquid−vapor interface in low concentration aqueous solutions. However, as in the case of surfactants, on increasing the concentration, amphiphiles tend to form micellar aggregates, which have interesting properties.[23] In this regard, there have been extensive studies on several micellar systems, such as those formed in aqueous sodium dodecyl sulfate (SDS), through experimental[24] and computational methods.[25]

The phase behavior of 1-*n*-decyl-3-methylimidazolium bromide ([C_{10}mim][Br]) has been studied by Firestone et al.[26] While imidazolium ionic liquids with longer alkyl chains (more than 12 carbons) are found to form a liquid crystalline phase, the ones with shorter alkyl chains (2−10 carbons) are isotropic liquids under ambient conditions. Firestone et al. found that by addition of 5−40% w/w water, a liquid crystalline gel phase forms at room temperature. However, in dilute aqueous solution, [C_{10}mim][Br] is found to form micelles that have been studied experimentally.[27]

Micelle formation of 1-alkyl-3-methylimidazolium bromide ionic liquids in aqueous solution has been studied using conductivity measurements and fluorescent probes[28] as well as UV absorption spectra.[29] Recent nuclear magnetic resonance (NMR) studies from Zhao and co-workers on a series of RTILs, [$C_n$mim][Br] with n equals 6, 8, 10, and 12 show the aggregation in their aqueous solutions.[30] They were able to derive the critical aggregation concentration (CAC) and the aggregation number for the various RTILs studied. According to their findings, except for [C_4mim][Br], all systems studied form aggregates in their aqueous solution, with CAC values ranging from 0.797 mol/kg for $n = 8$ to 0.011 mol/kg for $n = 12$. Moreover, they observed a dramatic decrease in CAC as the alkyl chain length was increased from 6 to 12. On the basis of their investigations, they proposed a possible structural model and also called for investigations by other methods for confirmation. In this regard, we have carried out atomistic level MD simulations of [C_{10}mim][Br] in bulk aqueous solution and also the liquid−vapor interface of this solution. We present details of simulations in the next section, followed by the results we have arrived at with discussion. We end with some conclusions derived from the present studies.

2. Methodology and Simulation Details

Classical MD simulations have been carried out on a bulk aqueous solution of [C_{10}mim][Br] using an explicit all atom force field model developed by Pádua and co-workers[31] using the PINY_MD code.[32] With 125 ion pairs and 6250 simple point charge (SPC) water molecules, the simulated system consisted of 24250 atoms. The bulk MD simulations in the canonical ensemble (constant NVT) were performed using three-dimensional periodic boundary conditions within a cubic box of edge length 62.08 Å at room temperature. Initial isothermal-isobaric (constant NPT) simulations performed at 1 atm of pressure were used to fix the density for the canonical ensemble simulations.

† Part of the "Max Wolfsberg Festschrift".

* To whom correspondence should be addressed. Phone: +1-215-573-8697. Fax: +1-215-573-6233. E-mail: bhargav@sas.upenn.edu (B.L.B.); klein@lrsm.upenn.edu (M.L.K.).

10.1021/jp8068865 CCC: $40.75
Published on Web 10/15/2008

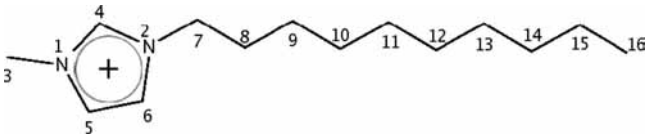

Figure 1. The [C_{10}mim] cation with the atom numbering scheme used in the discussion.

An Ewald summation method with an α value of 0.274 $Å^{-1}$ was used to compute electrostatic interactions,[33] and 19455 reciprocal space vectors were used to calculate the reciprocal space sum, which guaranteed convergence of the Coulomb energy. A Nosé-Hoover chain thermostat[34] was used to control the temperature of the system. The reversible reference system propagator (r-RESPA) algorithm,[35] a multiple time step method, was used to integrate the equations of motion. A time step of 3 fs was used to integrate nonbonded interactions beyond 6 Å and within 13 Å, while those nonbonded interactions within 6 Å were integrated with a time step of 1.5 fs. Torsional forces were evaluated every 0.75 fs, and stretching and bending degrees of freedom were evaluated with a time step of 0.375 fs. Nonbonded interactions were calculated up to a cutoff distance of 13 Å, and long-range corrections were applied for the calculation of energy and pressure tensor.

A separate MD simulation of an aqueous solution of [C_{10}mim][Br] with a vacuum interface has been performed. A pre-equilibrated aqueous solution (described above) was placed at the center of a supercell with edge lengths 62.08, 62.08, and 120Å thereby forming two vacuum−liquid interfaces. The α value and the number of reciprocal space vectors used for the Ewald summation were 0.271 $Å^{-1}$ and 36800, respectively, with other parameters remaining the same as mentioned above.

A dilute aqueous [C_{10}mim][Br] system was also constructed with a single ion pair in 2451 SPC water molecules. This system was simulated to study the behavior of dilute solution in bulk and at a vacuum−liquid interface. While the bulk system was simulated within a tetragonal box of 38.91, 38.91, and 48.64 Å along *X*, *Y*, and *Z* directions, respectively, the interface was simulated by placing the pre-equilibrated bulk system in a supercell of similar dimensions along *X* and *Y* directions but elongated in the *Z* direction to 90 Å to allow vacuum on both sides and to form two interfaces. The Ewald summation was carried out with α values of 0.262 and 0.272 $Å^{-1}$ for the bulk and interfacial systems, respectively.

All of the above-mentioned systems were equilibrated for 2 ns. The subsequent 8 ns trajectory was then stored at intervals of 0.9 ps and then used for analysis. The energy conservation (i.e., the sum of the physical energy of the system and the energy imparted from the thermostat variables) was monitored throughout and was found to be 1 part in 10^5 over 1 ns. A bin width of 1 Å was used in the calculation of density profiles, with the center of mass motion subtracted. Molecular graphics were rendered using VMD software.[36] A schematic drawing of the [C_{10} mim] cation is provided as Figure 1 to aid the discussion.

3. Results and discussion

The concentrated and dilute solutions studied by MD simulation correspond to 0.82 M and 16.7 mM, respectively. The observed mobility of the ions in these aqueous solutions was very high when compared to that in the pure ionic liquid.

3.1. Hydrogen Bonding. In both dilute and concentrated solutions, bromide ions are, on an average, surrounded by about seven water molecules and act as hydrogen-bond acceptors. Cation ring hydrogen atoms form hydrogen bonds with water, in which the carbon atoms of the ring act as donors. The water around the acidic hydrogen H(C_4) is somewhat more organized compared to that around the other two ring hydrogen atoms. On average, about half of the ring hydrogen atoms participate in hydrogen bonding. The presence of hydrogen bonds in pure ionic liquids and ionic liquid mixtures has been noted in previous MD simulation studies.[37,38] Experimental reports also confirm the presence of such hydrogen bonds in crystal structures of these ionic salts.[39,40] In aqueous solution, most of the direct H-bonds between the anion and cation (with carbon atom of the cation acting as donor and bromide ion as acceptor, respectively) are replaced with H-bonds to solvating water, which acts as a donor to bromide and acceptor in the case of the cation. In dilute solutions, solvation of ions is complete with no association between the ions, which is discussed later. However in concentrated solutions, the anion−cation interaction through a weak H bond persists partially. To identify strong hydrogen bonds, we employ a distance and angle cutoff of 2.5 Å and 160°, respectively, and for weak H bonds these values are 3.0 Å and 140°, respectively. While the anion forms strong H bonds with water, cation−anion and cation−water H bonds can be considered as weak. The numbers of H bonds present per cation and anion are presented in Table 1. The small increase in the number of anion−water H bonds in the case of dilute solution can be attributed to complete dissociation of anions.

TABLE 1: Average Number of Hydrogen Bonds Present per Ion in Different Systems Studied[a]

system	cation−water	cation−anion	anion−water
concentrated (bulk)	0.06 (1.37)	0.00 (0.04)	3.98 (6.39)
concentrated (interface)	0.06 (1.33)	0.00 (0.05)	3.96 (6.35)
dilute (bulk)	0.06 (1.43)	0.00 (0.00)	4.05 (6.62)
dilute (interface)	0.06 (1.34)	0.00 (0.00)	4.04 (6.60)

[a] Numbers in parentheses also include weak hydrogen bonds as defined in the text.

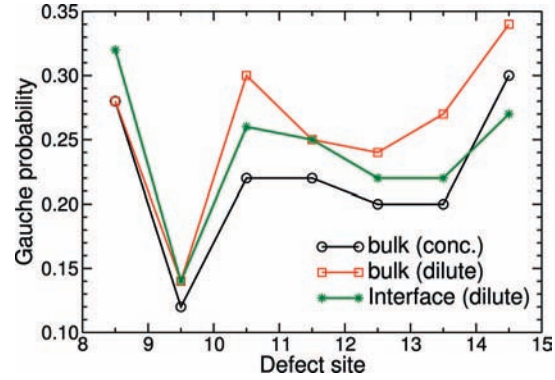

Figure 2. Shown is the gauche defect probability for torsion around different C−C bonds along the decyl chain. The gauche probability for the bond C_n C_{n+1} is plotted at (n + 0.5) with n referring to the atom numbering scheme presented in Figure 1. The statistical uncertainty in gauche defects is less than 1%.

3.2. Gauche Probability. The gauche defect probabilities for different C−C bonds of the cation tail are shown in Figure 2. There is significant probability for the alkyl chain to deviate from the all-trans conformation. The gauche defect probability is lowest for the bond between the carbon atoms C_9 and C_{10}. Water penetration has been observed around the headgroup as well as the beginning of the decyl chain which is in accordance with NMR results.[30] This might be the reason for observing low probability for gauche defects around C_9−C_{10}, as having a straight chain in that position would help to separate the tail and head (hydrophobic−hydrophilic separation). The defect

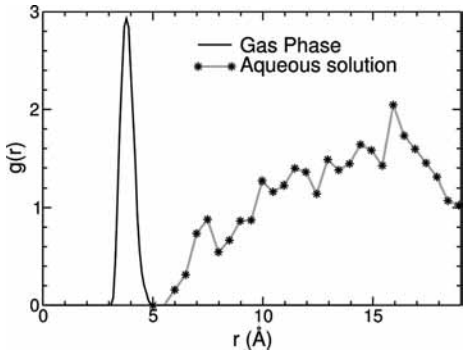

Figure 3. Radial distribution functions, $g(r)$ for bromide and the imidazolium cation obtained from MD simulations on a gas phase ion pair and on an aqueous solution with a single ion pair. The gas phase function has been scaled for comparison.

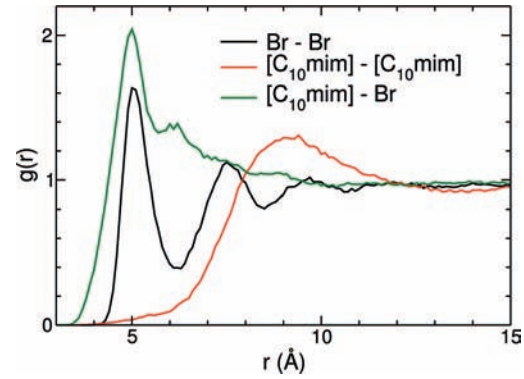

Figure 4. Radial distribution functions, $g(r)$ for anion−anion, cation−cation, and anion−cation obtained from MD simulation of the bulk aqueous solution of $[C_{10}mim][Br]$.

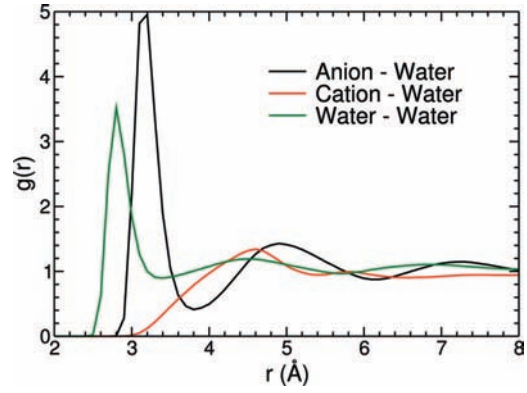

Figure 5. Radial distribution functions, $g(r)$ for anion−water, cation−water, and water−water obtained from MD simulation of the bulk aqueous solution of $[C_{10}mim][Br]$.

probability is larger for all other C−C bonds. In particular, both ends of the decyl chain show significantly enhanced probability for gauche defect formation. Among systems studied, defect probabilities are smaller in concentrated bulk solution followed by the dilute interface and are highest in the bulk dilute solution. From analyses of these defects, it can be concluded that the tail of the cation deviates from its linear all-trans configuration. This in turn has many implications in determining the orientation of cations near the liquid−vapor interface, which is discussed later.

3.3. Radial Distribution Functions. In the pure ionic liquid, various experimental and computational studies indicate association of the anions and cations. The radial distribution function (RDF) between the cation (imidazolium ring center) and anion is shown in Figure 3. It can be seen from the figure that although the anion is associated with the cation in the gas phase, in aqueous solution the ions are separated by solvent water. From analyses of site−site RDFs, it has been found that the bromide ion is associated with the acidic hydrogen of the imidazolium ring in the gas phase. Indeed, throughout the 10 ns MD simulation, the bromide ion was found within 5 Å of the acidic hydrogen and for more than 90% of the time within 3.5 Å, which can be considered an upper limit for the hydrogen bonding distance. It is evident from Figure 3 that the ions are separated in dilute aqueous solutions with negligible presence of an anion within 5 Å from the imidazolium ring center in the course of the 10 ns MD trajectory. The separation of ions by the solvent in dilute solution of RTIL has also been observed in a recent MD simulation of $[C_4mim][Cl]$.[41]

In the bulk MD simulations there are 125 ion pairs, and unlike the case of dilute solution, there is partial (39%) association of the anions with the cations. The observation in the MD simulations of full hydration of ions in dilute aqueous solutions and partial association in relatively concentrated aqueous solutions has also been reported from NMR experiments.[30]

Anion−anion, anion−cation, and cation−cation RDFs are shown in Figure 4. The cation position is defined as the center of imidazolium ring. The anion−anion RDF peaks at 5 Å with a first minimum at 6.3 Å as well as other distinct minima beyond the first minimum. The second and subsequent peaks in anion−anion RDF are due in part to organization of water around anions. The peak of the cation−anion RDF is also present at 5 Å with a small dip at 5.7 Å, but without any well-defined first minimum or any further oscillations before reaching the isotropic value of unity. The cation−cation RDF is rather broad, peaking at 9.3 Å without any further noticeable oscillations.

The RDFs for water around the anions and cations are presented in Figure 5 along with the water−water RDF. The anion−water RDF peak at 3.2 Å is narrow, suggesting strong ordering of water around the anions. This function has a minimum at 3.8 Å, which is followed by two more noticeable peaks with diminishing amplitude. Considering that the location of oxygen atom corresponds to the water in these functions, strong hydrogen bonding between anions and solvent water molecules is evident. The first hydration layer of bromide ion (up to first minimum in the RDF) contains 6.9 water molecules on an average. It can also be seen that the water is ordered in solution with the first peak position at 2.8 Å with around four nearest neighbor waters. Water ordering has also been observed, to a lesser extent, around the cation imidazolium rings.

The aggregation of cations due to their inherent amphiphilic nature is evident from Figure 6, which shows the RDFs for several sites on the cation with the same sites of other cations. It can be seen that the terminal carbon atom on the decyl chain is ordered to a great extent with a narrow peak at 4.2 Å. Segregation of polar and nonpolar regions of long alkyl chain imidazolium ionic liquids has been reported from previous computational[42,20] and experimental studies.[22] RDFs corresponding to C_4 (the carbon atom bonded to the acidic hydrogen) or C_8 (the second atom of decyl chain from the end attached to ring) does not show any peak suggesting strong ordering around each other. The spherical nature of the cation aggregates is also evident from the RDFs, which show the C_4 carbons lying further away from each other compared to the C_8 carbons.

3.4. Solution−vapor Interface. ***3.4.1. Dilute Solution.*** *Number Density Profiles.* Number density profiles for the cation, anion, and terminal methyl group of the decyl chain are shown in Figure 7 for dilute aqueous solution. Due to its amphiphilic nature, the cation is present at the interface with its headgroup

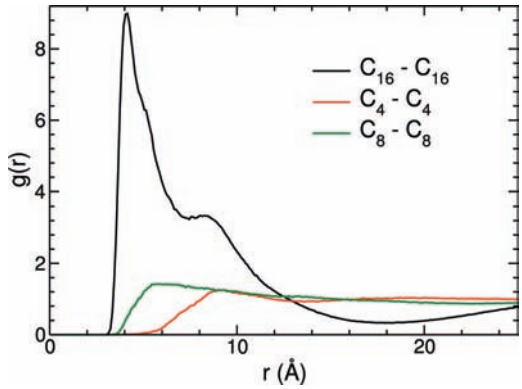

Figure 6. Radial distribution functions, $g(r)$ for C_4-C_4, C_8-C_8, and $C_{16}-C_{16}$ carbon atoms on different cations obtained from MD simulation of the bulk aqueous solution of [C_{10}mim][Br].

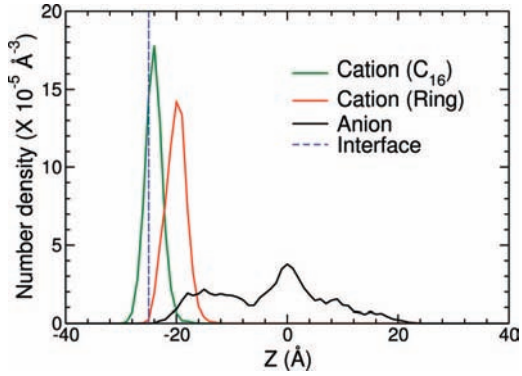

Figure 7. Number density profiles for the bromide anion, cation ring, and terminal methyl group of the decyl chain taken from an MD simulation of an ion pair in dilute aqueous [C_{10}mim][Br] solution.

in the water and tail at the interface. The counterion is mobile throughout the solution and does not have any preferred location. The interfacial boundary, represented in the figure by a blue dashed line, is defined as the region at which the density of water falls to half its bulk value. The green curve, representing the terminal methyl group density, lies at the interface but to the vacuum side of the cation headgroup distribution. The 4 Å separation in peak positions of these profiles for C_{16} and the ring center confirm that the decyl chain is not perpendicular to the interface otherwise the separation between peaks should have been much larger, i.e., 12 Å for an all-trans conformation.

3.4.2. Concentrated Solution. *Mass Density.* Since most of the cations are located at the vapor−liquid interface, it is not surprising that this is where an 8% increase in mass density over the bulk density is observed (data not shown). The bulk density fluctuates to a small extent due to the presence of micellar aggregates and is found to be around 1030 kg m^{-3}, whereas at the interface the density value is 1120 kg m^{-3}. Similar enhancement in mass and electron densities at the interface of pure ionic liquids has been observed experimentally[43] as well as via computational studies.[44]

Number Density. Number density profiles along the interface normal (Z axis) are shown in Figure 8. The red curve represents the profile for the centers of the imidazolium rings, whereas the green curve is the methyl group profile. The anion profile is indicated by a black line, and the water profile by a blue line. The latter has been scaled down by a factor of 50 for ease of comparison. Even though the mass density of the solution shows significant enhancement near the interface over the bulk value, the number density enhancement is almost negligible (data

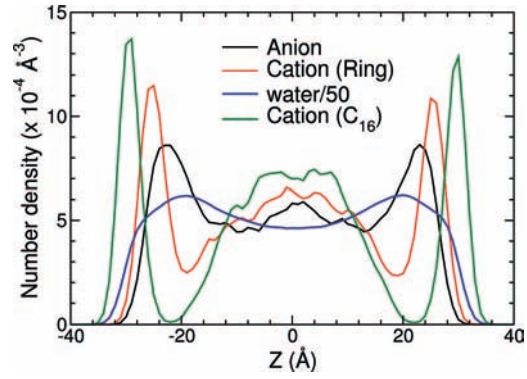

Figure 8. Number density profiles along the interface normal (Z direction) for bromide anions, cation rings, water, and terminal methyl groups taken from a MD simulation of a concentrated aqueous [C_{10}mim][Br] solution.

not shown). From the figure, it is clearly evident that cations have accumulated near the interface.

In the case of a pristine [C_4mim][PF_6] vapor−liquid interface studied using MD simulation, the terminal methyl group was found to extend out of the liquid region of the interface.[44] However, the organization was not to an extent found in the present studies. From the comparison of density profiles for the center of the imidazolium ring and the terminal methyl group, it can be concluded that the cation orients in such a way as to minimize the interaction of the hydrophobic alkyl chains with water. The anion is found to be present in the vicinity of the imidazolium ring, but within the water. Unlike in the pure [C_4mim][PF_6] liquid, where the anion number density was higher at the interface compared to bulk, in aqueous solution they tend to be present within the bulk region. Both the anion and cation number densities are higher near the center of the supercell. This increased density in the bulk of the solution is found to be due to formation of aggregates of cations, which will be discussed later. The number density of water does not vary much compared to that of the anions and cations but is certainly influenced by the presence of cation aggregates.

Cation Orientation. As seen from the density profiles, cations present at the interface are oriented such that most of alkyl tail does not interact with water, while at the same time the polar headgroup has favorable interactions with water. Since the orientation of the cation is not completely characterized by the density profiles, we examined the probability distributions for the orientation of three segments of the cation moiety. Shown in Figure 9 are selected orientational probabilities for the tail (a vector connecting the first and last carbon atoms of decyl chain) and headgroup (the N_1-N_2 and N_1-C_3 vectors) with respect to the interface normal (Z direction).

From the figure, the probability is highest for the alkyl tails to be tilted at an angle of around 50° to the interface normal. The probability is least to be parallel to the interface and in between to be aligned parallel to interface normal. However, it should be noted that the decyl tail is not perfectly linear, and due to kinks present (as observed from the gauche defect probability) the orientation of the tail can be more complicated.

In the case of the [bmim][PF_6] vapor−liquid interface, it was reported that butyl chains are parallel to interface normal.[44] The vector connecting two nitrogen atoms of the imidazolium ring has greater probability to be oriented along the interface normal, whereas the methyl group attached to the ring also has higher probability to be aligned perpendicular to interface on the opposite side. Even though there is significant probability for

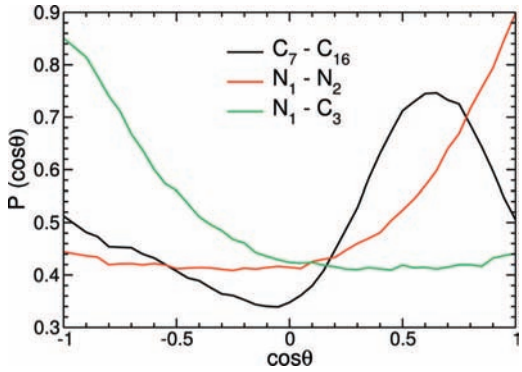

Figure 9. Orientation probability, $P(\cos\theta)$ with respect to the interface normal (Z direction), for the vectors C_7-C_{16}, N_1-N_2, and N_1-C_3, respectively, taken from MD simulations of the vapor−liquid interface of an aqueous $[C_{10}mim][Br]$ solution. Here, θ represents the angle between the Z direction and the aforementioned vectors.

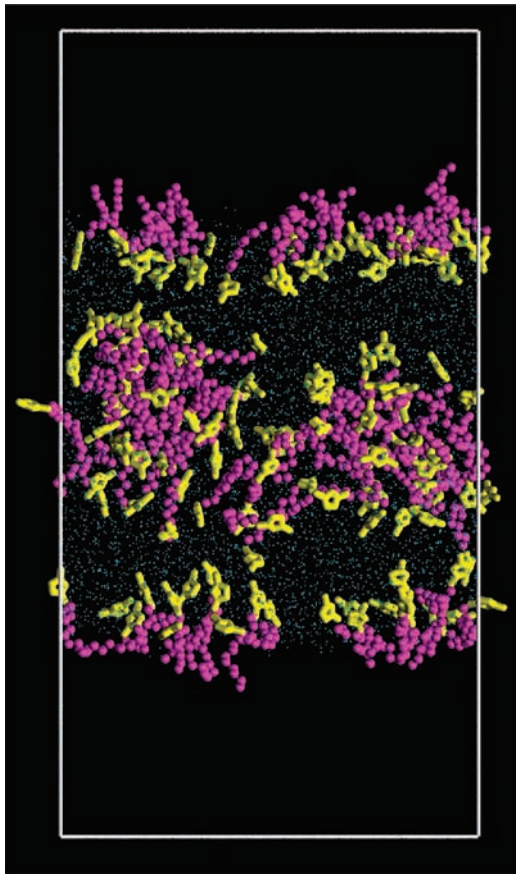

Figure 10. Snapshot of the aqueous $[C_{10}mim][Br]$ solution−vapor interface (side view with vapor above and below the solution slab) taken from a MD simulation. Atoms 1 through 7 of Figure 1, including the cation ring, are shown in yellow color, those numbered 8 through 16 in the cation tail are represented by magenta spheres, and the oxygen atoms of solvent water molecules are shown as cyan dots. Hydrogen and bromine atoms are not shown for clarity.

these two vectors to be aligned along a certain direction, they also occur in other orientations, which is evident from the figure.

Figure 10 shows a snapshot of the aqueous ionic liquid interface. In the figure the aggregation of the hydrophobic tails is clearly evident in the bulk regions and the tails are typically present at the interface lying horizontally on the surface of water with a small tilt. Even though some of the atoms of the tail are present in the water, the majority of the methyl and methylene groups tend to be present close to the interface. The headgroups

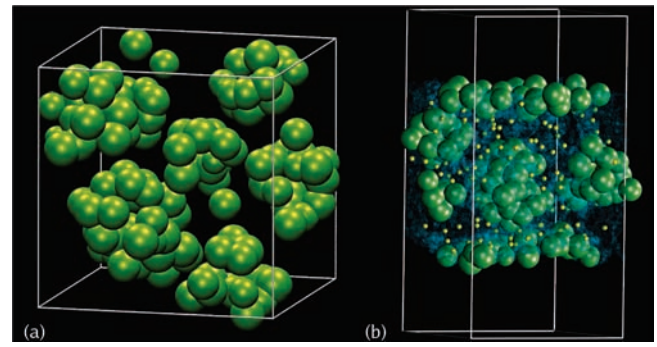

Figure 11. Cation aggregation: (a) Snapshot of the bulk aqueous system after 10 ns of MD. Cations are represented as beads. Water and anions are not shown for clarity. (b) Snapshot of the interfacial system after 10 ns of MD. Cations and anions are represented as beads in green and yellow color, respectively. Water is represented as a transparent blue density.

are present just below the interface, with the vector connecting the two N atoms parallel to surface normal (data not shown).

3.5. Aggregation. The MD simulations were started from a configuration in which the $[C_{10}mim]$ cations were uniformly distributed with bromide ions near imidazolium rings. During the course of the MD, small aggregates of cations spontaneously formed. A cation was identified as belonging to an aggregate if its terminal methyl group was within 9.0 Å from any other such methyl group in that aggregate. This distance was chosen after carefully visualizing the aggregates. Aggregates were typically quasi-spherical in shape, with the alkyl chain buried deep inside the aggregate and the imidazolium headgroup exposed to the aqueous environment (see Figure 10). Bromide ions were found to be distributed uniformly throughout the solution. Snapshots of the bulk and interfacial systems after 10 ns are shown in Figure 11.

Contribution of different interactions to the total intermolecular energy, including self- and cross terms between the headgroup, alkyl tail, anion, and water, during the evolution of the system was computed. It was found that while the electrostatic energy between the aforementioned pairs did not change much, huge change was observed in the van der Waals energy for the tail−tail interaction. We believe the favorable interactions between the alkyl chains leads to the process of aggregation in these solutions.

3.5.1. Aggregation Number. From Figure 11 it is clear that cation aggregates are not monodisperse. The presence of a few monomers has also been observed in the bulk, which is in accordance with experiment.[30] For the interfacial system, many of the cations are found near the water−vacuum interface with the imidazolium ring inside the aqueous region. Apart from these surface distributions, aggregates have also been found in the bulk region. In this system, all of the cations were observed to belong to one of the aggregates and there were no isolated monomers in the bulk phase of the aqueous solution. The cation number distribution at the interface converged within the first 1.5 ns of MD simulations with no further change thereafter. The average surface area per cation at the air−water interface was found to be 1.54 nm^2, which can be compared to the experimentally reported minimum area per ionic liquid molecule of 1.21 nm^2 for a similar ionic liquid, 1-*n*-decyl-3-methylpyridinium chloride.[45]

The fraction of cations present versus the size of the aggregates (in bulk solution) is shown in Figure 12. The data are averaged over the last 2 ns of the MD trajectory. Notice that aggregates are not monodisperse. From this figure it is clear

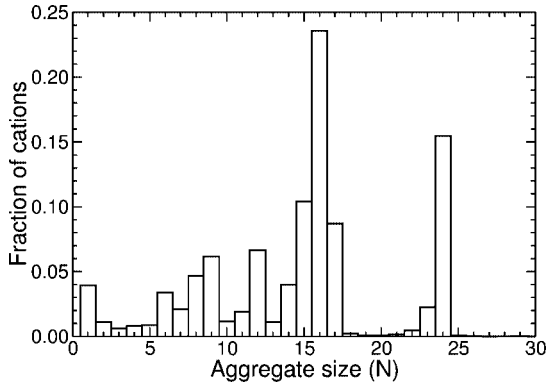

Figure 12. Fraction of cations involved in the formation of aggregates of different sizes. The data are averaged over the last 2 ns of the MD trajectory.

that apart from a few monomers, there are four aggregates with size ~16. There is also a small oligomer population with sizes less than 10. Apart from these, there is a micelle with size 24. The computed aggregation numbers were very sensitive to the definition, due to high ionic concentration and high mobility of the ions. During the course of simulation, monomers were found to be absorbed into the bigger aggregates and at the end of 10 ns simulations 70% of the cations in the bulk system were part of aggregates of sizes 16 or 24.

NMR data[30] has been interpreted using a model consisting of monomers and monodispersed aggregates and predict the aggregation number to be 27 for [C_{10}mim][Br] above the CAC. In another work,[27] based on the analysis of small-angle neutron scattering data, the variation of aggregation number with concentration of the solution gave the maximum aggregation number as 47 at a concentration of 0.6 mol/dm^{-3}. From the neutron data, the aggregation number looks almost saturated since it only increased from 45 to 47 on doubling the concentration from 0.3 to 0.6 M. The system we have studied has a concentration of 0.82 M, and thus the aggregation number should be at least 47.

Unfortunately, in the present MD studies, the time scale explored was limited to only 10 ns, and thus the system may well be in a metastable state with respect to the final state of cation aggregation. Although there was an initial rapid aggregation of the cations, the system did not evolve further by fusion of small aggregates. However, such a process cannot be ruled out.

3.5.2. Structure of Aggregates. With the knowledge of aggregation size distribution in the system, we can try to get some insight into the structure of these aggregates. A snapshot of one of the micelles is shown in Figure 13. Here the hydrogen atoms of the cations are omitted for clarity. Atoms shown in yellow color are those which form the polar headgroup region whereas atoms in magenta are of nonpolar alkyl tail region. It can be seen from the figure that the aggregate is quasi-spherical with nonpolar tail regions buried inside the aggregate favorably interacting via their van der Waals interactions and also minimizing unfavorable interactions with water. The cationic imidazolium rings are pointing radially outward toward water. Thus, the stairlike model proposed by Zhao et al.[30] for an aggregate of size 25 is highly unlikely based on the present MD simulations. In our studies, counterion bromides are not found inside any aggregates. Rather they are found dispersed isotropically in the solution.

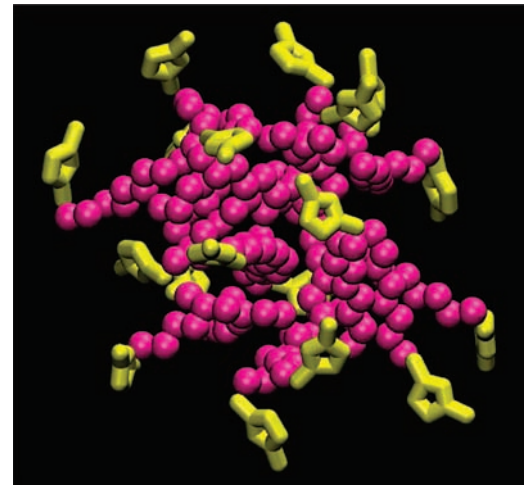

Figure 13. Snapshot of a micelle taken from the MD simulation of bulk [C_{10}mim][Br] in aqueous solution. Atoms represented with yellow color belong to polar headgroups and those represented with magenta belong to nonpolar alkyl tails. Hydrogen atoms, water, and counterions are not shown for clarity.

4. Conclusions

Aqueous solutions of [C_{10}mim][Br] have been studied using MD simulations. Starting from a uniform distribution of cations, evolution of the system to form small micellar aggregates has been observed. Oppositely charged ions, which are strongly associated in their neat liquid phase due to electrostatic interactions, are found to be associated completely in the gas phase, partially in concentrated aqueous solution and completely dissociated in dilute aqueous solutions, in accordance with experimental results.[41] The anion has been found to possess a well-defined solvation shell around it with about seven water molecules. Terminal methyl groups of cation decyl chains have been found to be localized inside micellar aggregates.

In dilute aqueous solutions, cations are likely to be found at the solution−vacuum interface with alkyl tails localized at the interface and headgroups lying inside water. Anions are not associated with cations and are free to wander throughout the system. In concentrated solution, excess cations, which cannot be accommodated at the interface, form micellar aggregates in the bulk solution. Even in concentrated solution, alkyl tails are present at the interface. However, anions are found to be present in the vicinity of the imidazolium ring.

The micellar aggregates are not monodisperse. The dominant aggregate sizes are found to be around 16 and 24. Monomers are also present in solution. The aggregation number of 24 is close to one of the experimentally determined aggregation numbers, namely, the value of 27 based on NMR and the monodisperse aggregate model.[30] The structure of the aggregate has been found to be quasi-spherical with nonpolar alkyl tails present at the center so as to avoid unfavorable interactions with water and the polar imidazolium rings present at the outer surface of the aggregates. The anions are found to be isotropically distributed throughout the system. The structure seen in MD simulations does not support a stairlike structure for [C_8mim][Br],[30] which seems unlikely due to unfavorable interactions between alkyl tails and water.

The model used for the present MD simulations has been successful in predicting the structure of several other ionic liquids[44] and thus seems likely to be reliable in the present context. However, experiments are often carried out at near CAC. Unfortunately, it is difficult to simulate at such low

concentrations of ionic liquids primarily because the number of water molecules that would have to be considered will be too large to make such simulations viable.

Another issue for the simulations is the time scale. Our MD simulation time is limited to around 10 ns, which is likely not enough for the system to explore the complete phase space for given state point. Accordingly, the observed broad distribution in the aggregation number may be due to this effect. This could be the reason that the present aggregation numbers are much less than those derived from small-angle neutron data. However, even with these limitations of system size and time scale, the present MD simulations are able to capture the spontaneous aggregation of [C_{10}mim][Br] starting from a random initial configuration. Given access to next generation computational resources, one might expect to observe formation of large numbers of small micellar aggregates that then fuse to form larger aggregates that dissociate and recombine before achieving an equilibrium distribution of micelle sizes. Clearly, long trajectory simulations on large systems will provide additional insight into the nature of the aggregates.

Acknowledgment. We thank Professor Balasubramanian Sundaram for helpful discussions. We thank the Ras Al Khaimah Center for Advanced Materials for supporting this work through a research fellowship named for His Highness Sheikh Saqr Bin Mohammed Al Qasimi.

References and Notes

(1) Welton, T. *Chem. Rev.* **1999**, *99*, 2071.
(2) Earle, M. J.; Seddon, K. R. *Pure Appl. Chem.* **2000**, *72*, 1391.
(3) Rogers, R. D.; Seddon, K. R. *Science* **2003**, *302*, 792.
(4) Swatloski, R. P.; Spear, S. K.; Holbrey, J. D.; Rogers, R. D. *J. Am. Chem. Soc.* **2002**, *124*, 4974.
(5) Haumann, M.; Riisager, A. *Chem. Rev.* **2008**, *108*, 1474.
(6) Kazarian, S. G.; Briscoe, B. J.; Welton, T. *Chem. Commun.* **2000**, 2047.
(7) Triolo, A.; Mandanici, A.; Russina, O.; Rodriguez-Mora, V.; Cutroni, M.; Hardacre, C.; Nieuwenhuyzen, M.; Bleif, H.; Keller, L.; Ramos, M. A. *J. Phys. Chem. B* **2006**, *110*, 21357.
(8) Kanakubo, M.; Umecky, T.; Hiejima, Y.; Aizawa, T.; Nanjo, H.; Kameda, Y. *J. Phys. Chem. B* **2005**, *109*, 13847.
(9) Hagiwara, R.; Hirashige, T.; Tsuda, T.; Ito, Y. *J. Fluorine Chem.* **1999**, *99*, 1.
(10) Hanke, C. G.; Price, S. L.; Lynden-Bell, R. M. *Mol. Phys.* **2001**, *99*, 801.
(11) Margulis, C. J.; Stern, H. A.; Berne, B. J. *J. Phys. Chem. B* **2002**, *106*, 12017.
(12) Lynden-Bell, R. M. *Mol. Phys.* **2003**, *101*, 2625.
(13) Del Popolo, M. G.; Voth, G. A. *J. Phys. Chem. B* **2004**, *108*, 1744.
(14) Wang, Y.; Voth, G. A. *J. Am. Chem. Soc.* **2005**, *127*, 12192.
(15) Hu, Z.; Margulis, C. J. *Proc. Natl. Acad. Sci. U.S.A.* **2006**, *103*, 831.
(16) Hunt, P. A. *Mol. Sim.* **2006**, *32*, 1.
(17) Bhargava, B. L.; Balasubramanian, S. *J. Phys. Chem. B* **2007**, *111*, 4477.
(18) Hunt, P. A. *J. Phys. Chem. B* **2007**, *111*, 4844.
(19) Hanke, C. G.; Lynden-Bell, R. M. *J. Phys. Chem. B* **2003**, *107*, 10873.
(20) Bhargava, B. L.; Devane, R.; Klein, M. L.; Balasubramanian, S. *Soft Matter* **2007**, *3*, 1395.
(21) Lopes, J. N. A. C.; Pádua, A. A. H. *J. Phys. Chem. B* **2006**, *110*, 3330.
(22) Triolo, A.; Russina, O.; Bleif, H.-J.; Di Cola, E. *J. Phys. Chem. B* **2007**, *111*, 4641.
(23) Torchilin, V. P.; Lukyanov, A. N.; Gao, Z.; Papahadjopoulos-Sternberg, B. *Proc. Natl. Acad. Sci. U.S.A.* **2003**, *100*, 6039.
(24) Rharbi, Y.; Winnik, M. A. *J. Am. Chem. Soc.* **2002**, *124*, 2082.
(25) Sammalkorpi, M.; Karttunen, M.; Haataja, M. *J. Phys. Chem. B* **2007**, *111*, 11722.
(26) Firestone, M. A.; Dzielawa, J. A.; Zapol, P.; Curtiss, L. A.; Seifert, S.; Dietz, M. L. *Langmuir* **2002**, *18*, 7258.
(27) Goodchild, I.; Collier, L.; Millar, S. L.; Prokeš, I.; Lord, J. C. D.; Butts, C. P.; Bowers, J.; Webster, J. R. P.; Heenam, R. K. *J. Colloid Interface Sci.* **2007**, *307*, 455.
(28) Vanyúr, R.; Biczók, L.; Miskolczy, Z. *Colloids Surf., A* **2007**, *299*, 256.
(29) Zhang, H.; Liang, H.; Wang, J.; Li, K. *Z. Phys. Chem.* **2007**, *221*, 1061.
(30) Zhao, Y.; Gao, S.; Wang, J.; Tang, J. *J. Phys. Chem. B* **2008**, *112*, 2031.
(31) (a) Lopes, J. N. C.; Deschamps, J.; Pádua, A. A. H. *J. Phys. Chem. B* **2004**, *108*, 2038. (b) Lopes, J. N. C.; Pádua, A. A. H. *J. Phys. Chem. B* **2006**, *110*, 19586.
(32) Tuckerman, M. E.; Yarne, D. A.; Samuelson, S. O.; Hughes, A. L.; Martyna, G. J. *Comput. Phys. Commun.* **2000**, *128*, 333.
(33) Allen, M. P.; Tildesley, D. J. *Computer Simulation of Liquids*; Clarendon: Oxford, 1987.
(34) Martyna, G. J.; Klein, M. L.; Tuckerman, M. E. *J. Chem. Phys.* **1992**, *97*, 2635.
(35) Tuckerman, M. E.; Berne, B. J.; Martyna, G. J. *J. Chem. Phys.* **1992**, *97*, 1990.
(36) Humphrey, W.; Dalke, A.; Schulten, K. *J. Mol. Graphics* **1996**, *14*, 33.
(37) Bhargava, B. L.; Balasubramanian, S. *Chem. Phys. Lett.* **2006**, *417*, 486.
(38) Bhargava, B. L.; Balasubramanian, S. *J. Phys. Chem. B* **2008**, *112*, 7566.
(39) Choudhury, A. R.; Winterton, N.; Steiner, A.; Cooper, A. I.; Johnson, K. A. *J. Am. Chem. Soc.* **2005**, *127*, 16792.
(40) Matsumoto, K.; Tsuda, T.; Hagiwara, R.; Ito, Y.; Tamada, O. *Solid State Sci.* **2002**, *4*, 23.
(41) Remsing, R. C.; Liu, Z.; Sergeyev, I.; Moyna, G. *J. Phys. Chem. B* **2008**, *112*, 7363.
(42) Wang, Y.; Voth, G. A. *J. Am. Chem. Soc.* **2005**, *127*, 12192.
(43) Sloutskin, E.; Ocko, B. M.; Tamam, L.; Kuzmenko, I.; Gog, T.; Deutsch, M. *J. Am. Chem. Soc.* **2005**, *127*, 7796.
(44) Bhargava, B. L.; Balasubramanian, S. *J. Am. Chem. Soc.* **2006**, *128*, 10073.
(45) Blesic, M.; Lopes, A.; Melo, E.; Petrovski, Z.; Plechkova, N. V.; Lopes, J. N. C.; Seddon, K. R.; Rebelo, L. P. N. *J. Phys. Chem. B* **2008**, *112*, 8645.

JP8068865